Fatigue assessment of steel rollers by means of the local energy

F. Chebat, M. Cincera
Rulli Rulmeca S.P.A., Via A. Toscanini, 1, I-24011 Alme' (Bergamo) – Italy

S.M.J. Razavi, F. Berto, T. Welo
Department of Mechanical and Industrial Engineering, Norwegian University of Science and Technology (NTNU), Norway
javad.razavi@ntnu.no, filippo.berto@ntnu.no

ABSTRACT. This paper aims to analyses the fatigue behavior of steel rollers using the average strain energy density (SED) criterion. Considering the variability of the V-notch opening angle, a simple scalar quantity, i.e. the value of the strain energy density averaged in a control volume surrounding the notch tip, has been introduced to overcome the complexities in failure assessment of this component. The strain energy is obtained using close form solutions based on the relevant Notch Stress Intensity Factors (NSIF) for modes I, II and III. Referring to the conventional arc welding processes, the radius of the control volume is carefully identified with reference to conventional arc welding processes being equal to 0.28 mm for welded joints made of steel. In this paper firstly the employed methodology for the fatigue assessment is described and then the first synthesis of fatigue data by means of local SED for a specific geometry is shown.

KEYWORDS. Notch Stress Intensity Factor; Welded Joints; Strain Energy Density; Fatigue Strength.

OPEN ACCESS

Citation: Chebat, F., Cincera, M. Razavi, S.M.J., Berto, F., Welo, T., Fatigue assessment of steel rollers by means of the local energy, Frattura ed Integrità Strutturale, 41 (2017) 447-455.

Received: 12.05.2017
Accepted: 24.05.2017
Published: 01.07.2017

INTRODUCTION

The geometry of weld fillet cannot be exactly defined due to variation of different parameters such as length of lack of penetration, root radius, toe radius and bead shape from joint to joint even in well-performed operations [1-5]. The weld toe radius decreases in presence of the local heat concentration during the welding process and it is considerably small for automated high-power processes such as laser beam welding. According to the small values of toe radius in conventional arc welding [6], the weld toe is considered as a sharp notch and using the NSIF approach the local stress can be obtained [6,7]. Considering the large opening angles of the weld toe, the stress component regarding to mode II is non-singular and the fatigue behaviour can be assessed only by use of mode I NSIF [7]. Based on the relevant theoretical stress concentration factors an evaluation of different steel welded joints can be conducted considering a fictitious notch

radius ρ_f =1.0 mm if the weld toe and root radius be considered as zero [8]. Fatigue failure is generally characterized by the nucleation and growth of cracks [9-13].
The difference between two stages of nucleation and growth of fatigue crack is "qualitatively distinguishable but quantitatively ambiguous" [14]. In this regard, NSIFs were used for prediction of crack nucleation and also the total fatigue life [15-19]. Prediction of the total fatigue life using NSIFs is only limited for the cases in which a large amount of fatigue life is consumed at short crack depth, within the zone governed by the notch singularity at the weld toe or root. Lassen [20] reported that up to 40 percent of fatigue life of transverse non-load-carrying fillet welded joints was related to nucleation of a microcrack with a length of 0.1 mm. Singh et al. [21,22] showed that 70 percent of the total fatigue life of fillet joints in AISI 304L was related to crack nucleation up to a size of 0.5 mm. According to the theoretical formulations related to the NSIF approach, this method cannot be employed for the joints characterized by weld flank angles very different from 135 degrees or for comparing failures at the weld root (2α =0°) or weld toe (2α =135°). That is due to the units which are used for mode I NSIF as MPa(m)$^{\beta}$, where the exponent β depends on the V-notch angle, according to the expression $\beta = 1-\lambda_1$, λ_1 being Williams' eigenvalue (Williams 1952). This problem was solved later by using the average strain energy density range present in a critical volume of radius R_c surrounding the weld toe or the weld root. Using some closed form formulations, the strain energy density range was defined as a function of the relevant NSIFs. The NSIF approach was later extended to welded joints under multiaxial loading [23]. The simple volume is approximately similar to that of proposed by Sheppard [24], while proposing a volume criterion based on local stresses to predict fatigue limits of notched components. Sonsino [25] proposed the highly stressed volume (the region where 90% of the maximum notch stress is exceeded) to predict the high cycle strength of welded joints. The same methodology based on strain energy is employed in this paper for fatigue analysis of streel rollers made by Rulmeca [26] with failure occurring at the weld root. The rollers studied in the present paper belong to the category PSV which is mainly suitable for conveyors that operate in very difficult conditions with high level of working loads where large lump size material is conveyed; and yet, despite these characteristics, they require minimal maintenance. The bearing housings of the PSV series are welded to the tube body using autocentralising automatic welding machines utilizing a continuous wire feed. Considering the fatigue behavior of the component, the weakest point of the entire structure is the lack of penetration of the weld root. Hence, if the roller is loaded well above its declared nominal admitted load [26] it would experience fatigue failure starting at the level of the weld root.
The current paper aims to describe the modelling method of the roller by using the finite element method combined with three-dimensional analyses (the procedure is described in more detail in [27] and implementation of the SED method in a control volume for two different tested geometries belonging to the family of rollers called PSV4 and characterized by a different lengths.

APPROACH BASED ON THE LOCAL SED: ANALYTICAL PRELIMINARIES

The degree of singularity of the stress fields due to re-entrant corners was established by Williams both for mode I and mode II loading [28]. When the weld toe radius ρ is set to zero, NSIFs quantify the intensity of the asymptotic stress distributions in the close neighbourhood of the notch tip. By using a polar coordinate system (r, θ) having its origin located at the sharp notch tip, the NSIFs related to mode I and mode II stress distribution are [29]:

$$K_1^N = \sqrt{2\pi}\lim_{r\to 0^+} r^{1-\lambda_1}\sigma_{\theta\theta}(r,\theta=0) \tag{1}$$

$$K_2^N = \sqrt{2\pi}\lim_{r\to 0^+} r^{1-\lambda_2}\tau_{r\theta}(r,\theta=0) \tag{2}$$

where the stress components $\sigma_{\theta\theta}$ and $\tau_{r\theta}$ have to be evaluated along the notch bisector (θ = 0).
Dealing with mode III loading an extension of the definition proposed by Gross and Mendelson [29] has been carried out in [30,31]:

$$K_3^N = \sqrt{2\pi}\lim_{r\to 0^+} r^{1-\lambda_3}\tau_{\theta z}(r,\theta=0) \tag{3}$$

By means of Eqs. (1,2), it is possible to present Williams' formulae for stress components as explicit functions of the NSIFs. Then, mode I stress distribution is [32]:

$$\left\{\begin{matrix}\sigma_{\theta\theta}\\ \sigma_{rr}\\ \tau_{r\theta}\end{matrix}\right\}_{\rho=0}=\frac{1}{\sqrt{2\pi}}\frac{r^{\lambda_1-1}K_1^N}{(1+\lambda_1)+\chi_1(1-\lambda_1)}\left[\left\{\begin{matrix}(1+\lambda_1)\cos(1-\lambda_1)\theta\\ (3-\lambda_1)\cos(1-\lambda_1)\theta\\ (1-\lambda_1)\sin(1-\lambda_1)\theta\end{matrix}\right\}+\chi_1(1-\lambda_1)\left\{\begin{matrix}\cos(1+\lambda_1)\theta\\ -\cos(1+\lambda_1)\theta\\ \sin(1+\lambda_1)\theta\end{matrix}\right\}\right] \tag{4}$$

Mode II stress distribution is:

$$\left\{\begin{matrix}\sigma_{\theta\theta}\\ \sigma_{rr}\\ \tau_{r\theta}\end{matrix}\right\}_{\rho=0}=\frac{1}{\sqrt{2\pi}}\frac{r^{\lambda_2-1}K_2^N}{(1-\lambda_2)+\chi_2(1+\lambda_2)}\left[\left\{\begin{matrix}-(1+\lambda_2)\sin(1-\lambda_2)\theta\\ -(3-\lambda_2)\sin(1-\lambda_2)\theta\\ (1-\lambda_2)\cos(1-\lambda_2)\theta\end{matrix}\right\}+\chi_2(1+\lambda_2)\left\{\begin{matrix}-\sin(1+\lambda_2)\theta\\ \sin(1+\lambda_2)\theta\\ \cos(1+\lambda_2)\theta\end{matrix}\right\}\right] \tag{5}$$

Mode III stress distribution is:

$$\begin{aligned}\tau_{zr}&=\frac{K_3^N}{\sqrt{2\pi}}r^{\lambda_3-1}\sin(\lambda_3\theta)\\ \tau_{z\theta}&=\frac{K_3^N}{\sqrt{2\pi}}r^{\lambda_3-1}\cos(\lambda_3\theta)\end{aligned} \tag{6}$$

All stress and strain components in the highly stressed region are correlated to mode I, mode II and mode III NSIFs. Under plane strain hypothesis, the strain energy included in a semicircular sector is [33,34]:

$$\Delta\bar{W}=\frac{e_1}{E}\left[\frac{\Delta K_1^N}{R_C^{1-\lambda_1}}\right]^2+\frac{e_2}{E}\left[\frac{\Delta K_2^N}{R_C^{1-\lambda_2}}\right]^2+\frac{e_3}{E}\left[\frac{\Delta K_3^N}{R_C^{1-\lambda_3}}\right]^2 \tag{7}$$

where R_C is the radius of the semicircular sector and e_1, e_2 are functions that depend on the opening angle 2α and on the Poisson's ratio ν, while e_3 depends only on the notch opening angle. A rapid calculation, with $\nu = 0.3$, can be made for e_1 and e_2 by using the following expressions [33]:

$$e_1=-5.373\cdot10^{-6}(2\alpha)^2+6.151\cdot10^{-4}(2\alpha)+0.1330 \tag{8}$$

$$e_2=4.809\cdot10^{-6}(2\alpha)^2-2.346\cdot10^{-3}(2\alpha)+0.3400 \tag{9}$$

where 2α is in degrees. Dealing with failures originated at the crack tip (i.e. weld root) Eq. (7) can be simplified as follows:

$$\Delta\bar{W}=\frac{1}{ER_C}\left[e_1\Delta K_1^2+e_2\Delta K_2^2+e_3\Delta K_3^2\right] \tag{10}$$

The material parameter R_C can be estimated by using the fatigue strength $\Delta\sigma_A$ of the butt ground welded joints (in order to quantify the influence of the welding process, in the absence of any stress concentration effect) and the NSIF-based fatigue

strength of welded joints having a V-notch angle at the weld toe constant and large enough to ensure the non singularity of mode II stress distributions. A convenient expression is [33]:

$$R_C = \left(\frac{\sqrt{2e_1}\ \Delta K_{1A}^N}{\Delta \sigma_A} \right)^{\frac{1}{1-\lambda_1}} \tag{11}$$

where both λ_1 and e_1 depend on the V-notch angle. Eq. (11) will be applied in the next sections of the paper taking into account the experimental value ΔK_{1A}^N at 5 million cycles related to transverse non-load carrying fillet welded joints with 2α = 135 degrees at the weld toe. The hypothesis of constancy of R_C under mixed mode loads had been validated by Lazzarin and Zambardi [33] by using experimental data mainly provided by Seweryn et al. [35] and Kihara and Yoshii [36]. From a theoretical point of view the material properties in the vicinity of the weld toes and the weld roots depend on a number of parameters as residual stresses and distortions, heterogeneous metallurgical micro-structures, weld thermal cycles, heat source characteristics, load histories and so on. To device a model capable of predicting R_C and the fatigue life of welded components on the basis of all these parameters is really a task too complex. Thus, the spirit of this approach is to give a simplified method able to summarise the fatigue life of components only on the basis of geometrical information, treating all other effects only in statistical terms, with reference to a well-defined group of welded materials and, for the time being, to arc welding processes. Eq. (11) makes it possible to estimate the R_C value as soon as ΔK_{1A}^N and $\Delta\sigma_A$ are known. At N_A = $5{\cdot}10^6$ cycles and in the presence of a nominal load ratio R equal to zero, a mean value ΔK_{1A}^N equal to 211 MPa.mm$^{0.326}$ can be assumed [37]. For butt ground welds made of ferritic steels Atzori and Dattoma [38] found a mean value $\Delta\sigma_A$ = 155 MPa (at $N_A = 5\times10^6$ cycles, with R=0). That value is in very good agreement with $\Delta\sigma_A$ =153 MPa recently obtained by Taylor at al. [5] by testing butt ground welds fabricated of a low carbon steel. Then, by introducing the above mentioned value into Eq. (11), one obtains for steel welded joints with failures from the weld toe R_C =0.28 mm. The choice of 5 million cycles as a reference value is due mainly to the fact that, according to Eurocode 3, nominal stress ranges corresponding to 5 million cycles can be considered as fatigue limits under constant amplitude load histories. It is worth noting that the simplified hypothesis of a semicircular core of radius R_C led to the assessment of a fatigue scatter band that exactly agreed with that of Haibach's normalised S-N band [39]. In the case 2α= 0 and fatigue crack initiation at the weld root Eq. (11) gives R_C = 0.36 mm, by neglecting the mode II contribution and using e_1 = 0.133, Eq. (8), ΔK_{1A}^N = 180 MPa mm$^{0.5}$ and, once again, $\Delta\sigma_A$ = 155 MPa. There is a small difference with respect to the value previously determined, R_C = 0.28 mm. However, in the safe direction, the proposal is to use R_C = 0.28 mm also for the welded joints with failures from the weld roots which is the case considered in the present manuscript. As opposed to the direct evaluation of the NSIFs, which needs very refined meshes, the mean value of the elastic SED on the control volume can be determined with high accuracy by using coarse meshes [40-43].

MODELLING OF THE ROLLERS AND EVALUATION OF THE LOCAL SED

The rollers considered in the present investigation belong to the series PSV which offer the highest quality and the maximum load capacity of Rulmeca's production (see Fig. 1) [26].

Rollers PSV are particularly suited to conveyors that operate in very difficult conditions, where working loads are high, and large lump size material is conveyed; and yet, despite these characteristics, they require minimal maintenance. Typical types of application are: mines, caves, cement works, coal-fired electric utilities and dock installations. The effectiveness of the PSV roller sealing system provides the solution to the environmental challenges of dust, dirt, water, low and high temperatures.

Roller is made of the following main components:

- A mantel, constituted by a tube cut and machined using automatic numerically controlled machines, which guarantee and maintain the tolerances and the precision of the square cut.
- Two bearing housing made by a steel monolithic structure (in agreement with UNI EN 10111 characterized by a yield strength $170<\sigma_y<330$ MPa), deep drawn and sized to a forced fixed tolerance (ISO M7) at the bearing position. The thickness of the housings is proportional to the spindle diameter and to the bearing type, with thicknesses that are up to 5 mm, to guarantee the maximum strength for each application, including the heaviest.

- A spindle which sustains the roller when it is assembled into the troughing set supports. It is made from drawn steel, cut and machined by automatic numerically controlled machines. The spindle is ground to a precision tolerance, to guarantee a perfect match of bearings, seals. Spindle tolerance, together with bearing housing tolerances, functionally guarantees the autoalignment of the internal and outer bearing rings of the ball race resulting in a good performance even when the spindle deflection is extreme due to overloading.
- The seals components, which are meant to protect the bearing from harmful elements that may impinge from the outside or the inside of the roller, made of three main sections:

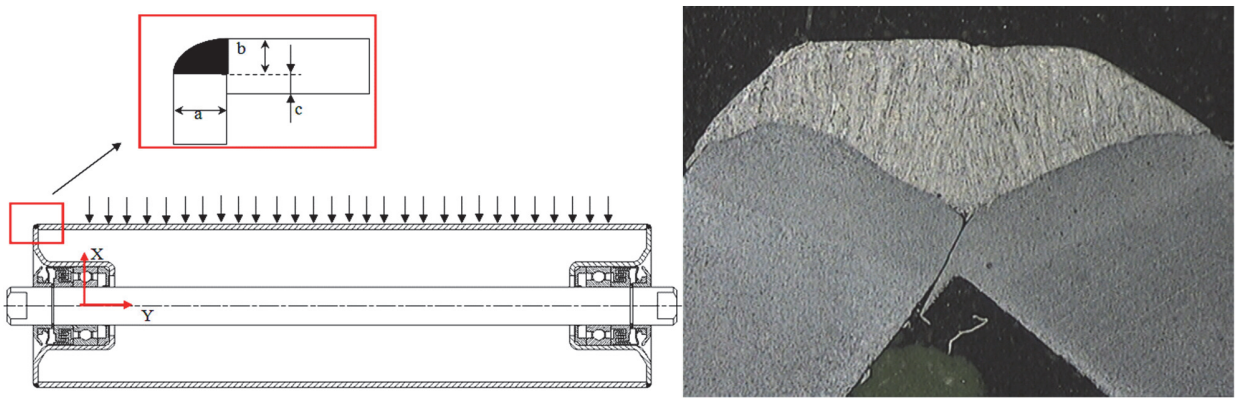

Figure 1: Scheme showing the main geometrical parameters at the weld root and an example of lack of penetration.

- Two bearing housing made by a steel monolithic structure (in agreement with UNI EN 10111 characterized by a yield strength $170<\sigma_y<330$ MPa), deep drawn and sized to a forced fixed tolerance (ISO M7) at the bearing position. The thickness of the housings is proportional to the spindle diameter and to the bearing type, with thicknesses that are up to 5 mm, to guarantee the maximum strength for each application, including the heaviest.
- A spindle which sustains the roller when it is assembled into the troughing set supports. It is made from drawn steel, cut and machined by automatic numerically controlled machines. The spindle is ground to a precision tolerance, to guarantee a perfect match of bearings, seals. Spindle tolerance, together with bearing housing tolerances, functionally guarantees the autoalignment of the internal and outer bearing rings of the ball race resulting in a good performance even when the spindle deflection is extreme due to overloading.
- The seals components, which are meant to protect the bearing from harmful elements that may impinge from the outside or the inside of the roller, made of three main sections:
  1. external section: made of an external stone guard, a lip ring made from soft anti-abrasive rubber with a large contact surface onto a metal cover cap; that forms a self-cleaning stage of seal in that it centrifugally repels water and dust naturally towards the outside;
  2. outward bearing protection: triple lip labyrinth in nylon PA6 greased to give further bearing protection;
  3. inward bearing protection, made of a sealing ring in nylon PA6 is positioned that provides an ample grease reservoir and also retains the grease near to the bearing even when there is a depression due to an abrupt change in temperature (pumping effect).
- Locking system: provided by means of the correctly located cir-clip, which is the most effective and the strongest system implemented in heavy rollers for belt conveyors.

The feature under investigation in this paper is the joint between tube and bearing housing.

The bearing housings of the PSV rollers are welded to the tube body using autocentralising automatic welding machines utilising a continuous wire feed. Tube and bearing housing form a monolithic structure of exceptional strength which itself reduces to the minimum any imbalance in the roller. This guarantees the alignment and concentricity with respect to the external diameter of the component parts of the sealing system. The optimum balance and concentricity thus obtained allows these rollers to be used at the highest speeds, eliminating harmful vibration to the conveyor structure and the "hammer effect" on the bearings of the rollers.

From the point of view of the fatigue behavior under loading, the weakest point of the entire structure is the lack of penetration of the weld root. Therefore, if the roller is loaded well above its declared nominal admitted load [26] it would experience fatigue failure starting at the level of the weld root. A detail of the weld root is shown in Fig. 1, where the lack

of penetration length is indicated as *c*. The load on top of the roller is modelled typically as a uniformly distributed load on the longitudinal line of the roller.

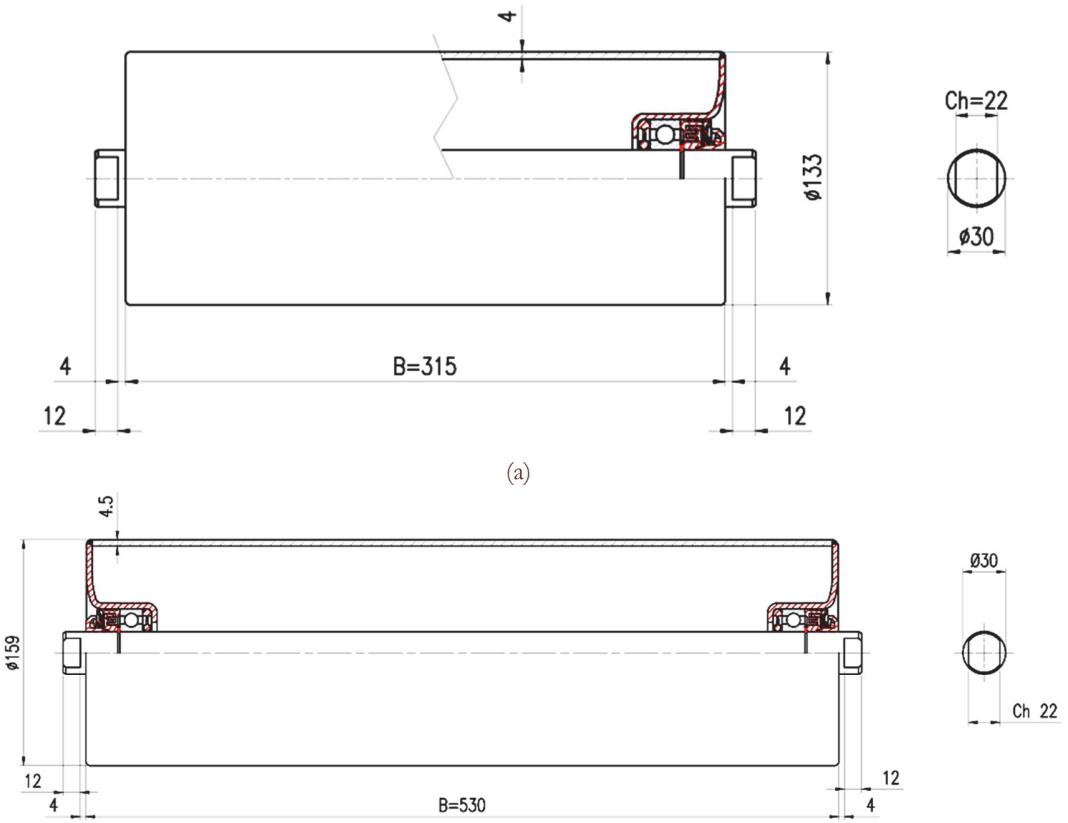

Figure 2: Geometry of the rollers: PSV4 133 315 (a) PSV4 159 530 (b).

Two geometries have been considered here and the details of the geometrical parameters are reported in Fig. 2a and 2b for the two cases, named in the following as PSV4 133 315 and PSV4 159 530. For sake of brevity the modeling will be shortly described only for the first geometry. Further details are reported in [27].

The analysis of the stress fields in these welded details needed 3D models, because of their variability along the circular path described by the weld root. The two considered geometries reported in Fig. 2 have been modelled by means of 20-node 3D finite elements implemented in the FE code ANSYS. Due to the symmetry of geometry and loading only one quarter of the geometry has been considered. The bearing has been considered of infinite stiffness and all the nodes of the bearing housing have been connected by means of rigid elements (links) to a master node. This special node has been placed on the symmetrical longitudinal axis of the roller in correspondence of the instantaneous rotation centre of the bearing. The rotation about the axis Z (ROT_Z) and the longitudinal displacement (U_Y, see Fig. 1) have been left unconstrained, while all other displacements and rotations of the master node have been constrained. The load has been distributed along the longitudinal line.

For each geometry two models were created: the first was mainly oriented to the determination of the point where the maximum principal stress and the maximum value of the strain energy density were located. Due to the complex geometry of the bearing housing in fact the point varies as a function of the geometry. In this case a regular fine mesh has been used with the aim also to determine the SIFs at the weld root.

The second model was characterized by a coarse mesh but by an accurate definition of the control volume where the strain energy density should be averaged. As just stated the mesh used in that case was coarse with a regular increasing spacing ratio in the direction of the position of the control volume mainly aimed to a correct positioning of the volume itself in the most critical region. All FE analyses have been carried out by means of 20-node finite elements under linear-elastic hypotheses.

FATIGUE STRENGTH IN TERMS OF STRAIN ENERGY DENSITY AVERAGED IN A FINITE SIZE VOLUME

By using the first model with a regular and very fine mesh the SED has been evaluated circumferentially all around the roller in the zone surrounding the weld root. The maximum SED value occurs outside the line of the application of the load. The angle of rotation is strongly dependent on the geometry of the bearing housing. In the case of the roller PSV 133 315 the maximum SED occurs at about 30 degrees from the line of load application. In that point all the modes of failure are contemporary present as will be discussed in the following.

For this specific model an analysis of sensitivity of SED as a function of the length of the lack of penetration c has been carried out [27]. From a micrographic analysis conducted on a large amount of welded rollers c has been found to vary in the range between 0.6 and 1.0 mm. A typical image of the weld root is shown in Fig. 1b. The sensitivity analysis has been made varying the length of the lack of penetration and evaluating the SED in a control volume of radius R_C = 0.28 mm. The variation of the SED is very limited in the range of c considered. The SED varies from 0.31 MJ/m^3 to 0.35 MJ/m^3 for a value of c corresponding to 0.6 and 1.0 mm, respectively. Considering the low variation of the SED as a function of the initial lack of penetration, the length c = 1 mm has been set in all FE analyses. This choice is in the safe direction because the worst configuration has been considered.

Some fatigue tests have been conducted on the two rollers shown in Fig. 2 [27]. A test system has been created for reproducing the service conditions on the roller. The load has been applied by means of an external counter-roll which press with a constant pressure the tested roller which rotates with a regular speed. Altogether 22 new tests have been carried out considering the two investigated geometries. The new results reconverted in terms of the local SED have been compared with the scatterband proposed for structural welded steels [36]. That band is shown in Fig. 3 together with the new data. It is evident that the previous scatter band can be satisfactorily applied also to the new data from failure at the weld root of rollers tested at different load levels.

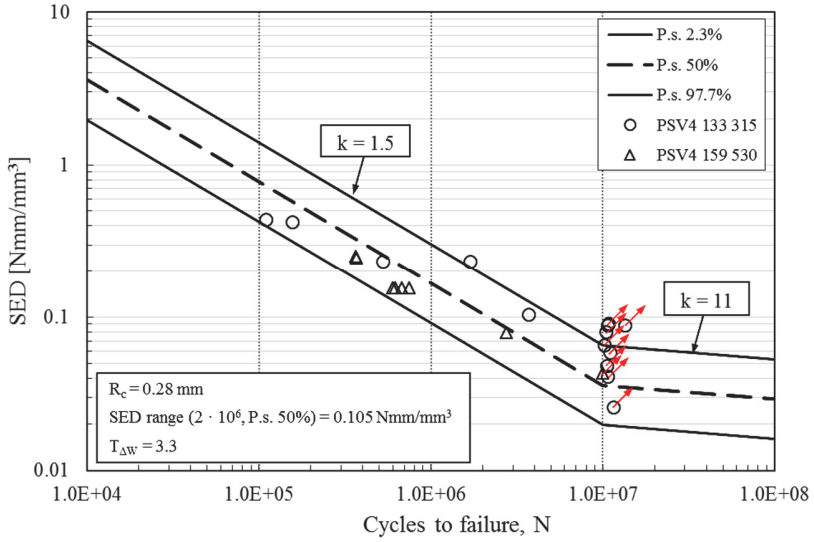

Figure 3: Synthesis of new data in terms of local SED and comparison with the scatterband by Lazzarin and co-authors.

CONCLUSIONS

The present paper deals with a local energy based approach employed for the fatigue assessment of rollers with failure occurring at the weld root. The rollers considered in the present investigation are particularly suited to conveyors that operate in very difficult conditions, where working loads are high, and large lump size material is conveyed; and yet, despite these characteristics, they require minimal maintenance. The bearing housings are welded to the tube body using autocentralising automatic welding machines utilizing a continuous wire feed.

From the point of view of the fatigue behavior under loading, the weakest point of the entire structure is the lack of penetration of the weld root. Therefore, if the roller is loaded well above its declared nominal admitted load [26], it would

experience fatigue failure starting at the level of the weld root. A detail of the weld root is shown in Fig. 1b, where the lack of penetration length is indicated as *c*.

The rollers have been modelled by using the finite element method combined with three-dimensional analyses. The procedure for evaluating the local parameters in the zone close to the lack of penetration at the weld root has been described in the paper showing the low sensitivity of the model to the length of the lack of penetration. The detailed procedure for evaluating the SED in the control volume surrounding the crack tip in the weakest point of the roller has been summarised [27]. Some fatigue tests from two different geometries belonging to the family of rollers called PSV4 from Rulmeca production have been carried out and summarised here by means of local SED. It has been proved that the scatter band ΔW-N (strain energy range – number of cycles to failure), summarising about 1200 fatigue data from welded joints with the majority of failures originated from the weld toes, can be successfully applied also to welded joints with failures from the weld roots and in particular to the considered rollers geometry.

REFERENCES

[1] Zou, L., Yang, X., Tan, J., Sun, Y., S-N curve modeling method of aluminum alloy welded joints based on the fatigue characteristics domain, Frattura ed Integrita Strutturale, 11(40) (2017) 137-148.

[2] Abe, T., Akebono, H., Kato, M., Sugeta, A., Fatigue properties and fracture mechanism of load carrying type fillet joints with one-sided welding, Frattura ed Integrita Strutturale, 10(35) (2016) 196-205.

[3] Tsutsumi, S., Morita, K., Fincato, R., Momii, H., Fatigue life assessment of a non-load carrying fillet joint considering the effects of a cyclic plasticity and weld bead shape, Frattura ed Integrita Strutturale, 10(38) (2016) 244-250.

[4] Radaj, D., Design and analysis of fatigue resistant welded structures, Abington Publishing, Cambridge (1990).

[5] Taylor, D., Barrett, N., Lucano, G., Some new recent methods for predicting fatigue in welded joints, Int. J. Fatigue, 24 (2002) 509-518.

[6] Yakubovskii, V.V., Valteris, I.I., Geometrical parameters of butt and fillet welds and their influence on the welded joints fatigue life, International Institute of Welding, Document XIII-1326-89 (1989).

[7] Dunn, M.L., Suwito, W., Cunningham, S., Fracture initiation at sharp notches: Correlation using critical stress intensities, Int. J. Solids Struct., 34 (1997) 3873-3883.

[8] Lazzarin, P., Tovo, R., A Notch Intensity Approach to the Stress Analysis of Welds, Fatigue Fract. Eng. Mater. Struct. 21 (1998) 1089-1104.

[9] Ayatollahi, M.R., Razavi, S.M.J., Chamani, H.R., Fatigue Life Extension by Crack Repair Using Stop-hole Technique under Pure Mode-I and Pure mode-II Loading Conditions, Procedia Eng., 74 (2014) 18–21.

[10] Ayatollahi, M.R., Razavi, S.M.J., Chamani, H.R., A numerical study on the effect of symmetric crack flank holes on fatigue life extension of a SENT specimen, Fatigue Fract. Eng. Mater. Struct. 37(10) (2014) 1153-1164.

[11] Ayatollahi, M.R., Razavi, S.M.J., Yahya, M.Y., Mixed mode fatigue crack initiation and growth in a CT specimen repaired by stop hole technique, Eng. Fract. Mech. 145 (2015) 115-127.

[12] Ayatollahi, M.R., Razavi, S.M.J., Sommitsch, C., Moser, C., Fatigue life extension by crack repair using double stop-hole technique, Mater. Sci. Forum, 879 (2017) 3-8.

[13] Razavi, S.M.J., Ayatollahi, M.R., Sommitsch, C., Moser, C., Retardation of fatigue crack growth in high strength steel S690 using a modified stop-hole technique, Eng. Fract. Mech., 169 (2017) 226–237.

[14] Jiang, Y., Feng, M., Modeling of fatigue crack propagation, J. Eng. Mater. Technol., 126 (2004) 77-86.

[15] Berto, F., Lazzarin, P., Recent developments in brittle and quasi-brittle failure assessment of engineering materials by means of local approaches, Mater. Sci. Eng. R, 75 (2014) 1–48.

[16] Ferro, P., The local strain energy density approach applied to pre-stressed components subjected to cyclic load, Fatigue Fract. Eng. Mater. Struct. 37 (2014) 1268–1280.

[17] Radaj, D., State-of-the-art review on the local strain energy density concept and its relation to the J-integral and peak stress method, Fatigue Fract. Eng. Mater. Struct., 38 (2015) 2–28.

[18] Radaj, D., Berto, F., Lazzarin, P., Local fatigue strength parameters for welded joints based on strain energy density with inclusion of small-size notches, Eng. Fract. Mech., 76 (8) (2009) 1109-1130.

[19] Lazzarin, P., Campagnolo, A., Berto, F., A comparison among some recent energy- and stress-based criteria for the fracture assessment of sharp V-notched components under mode I loading, Theor. Appl. Fract. Mech., 71 (2014) 21-30.

[20] Lassen, T., The effect of the welding process on the fatigue crack growth. Welding J. 69, Research Supplement, (1990) 75S-81S.

[21] Singh, P.J., Achar, D.R.G., Guha, B., Nordberg H., Fatigue life prediction of gas tungsten arc welded AISI 304L cruciform joints different LOP sizes, Int. J. Fatigue, 25 (2003) 1-7.
[22] Singh, P.J., Guha, B., Achar, D.R.G., Nordberg, H., Fatigue life prediction improvement of AISI 304L cruciform welded joints by cryogenic treatment, Eng. Fail. Anal. 10 (2003) 1-12.
[23] Lazzarin, P., Sonsino, C.M., Zambardi, R., A Notch Stress Intensity approach to predict the fatigue behaviour of T butt welds between tube and flange when subjected to in–phase bending and torsion loading, Fatigue Fract. Eng. Mater. Struct. 27 (2004) 127-141.
[24] Sheppard, S.D., Field effects in fatigue crack initiation: long life fatigue strength. Trans. ASME, J. Mech. Design 113 (1991) 188-194.
[25] Sonsino, C.M., Multiaxial fatigue of welded joints under in-phase and out-of-phase local strains and stresses, Int. J. Fatigue 17 (1995) 55-70.
[26] Rulmeca Bulk Catalogue, 2014
[27] Berto, F., Campagnolo, A., Chebat, F., Cincera, M., Santini, M., Fatigue strength of steel rollers with failure occurring at the weld root based on the local strain energy values: modelling and fatigue assessment, Int. J. Fatigue, 82 (2016) 643–657.
[28] Williams, M.L., Stress singularities resulting from various boundary conditions in angular corners of plates in extension, J. Appl. Mech. 19 (1952) 526-528.
[29] Gross, R., Mendelson, A., Plane Elastostatic Analysis of V-Notched Plates, Int. J. Fract. 8 (1972) 267-276.
[30] Qian, J., Hasebe, N., Property of eigenvalues and eigenfunctions for an interface V-notch in antiplane elasticity, Eng. Fract. Mech. 56 (1997) 729–734.
[31] Zappalorto, M., Lazzarin, P., Yates, J.R., Elastic stress distributions resulting from hyperbolic and parabolic notches in round shafts under torsion and uniform antiplane shear loadings, Int. J. Solid. Struct., 45 (2008) 4879-4901.
[32] Lazzarin, P., Tovo R., A unified approach to the evaluation of linear elastic fields in the neighbourhood of cracks and notches, Int. J. Fract., 78 (1996) 3-19.
[33] Lazzarin, P., Zambardi, R., A finite-volume-energy based approach to predict the static and fatigue behaviour of components with sharp V-shaped notches, Int. J. Fract. 112 (2001) 275-298.
[34] Berto, F., Campagnolo, A., Lazzarin, P., Fatigue strength of severely notched specimens made of Ti–6Al–4V under multiaxial loading, Fatigue Fract. Eng. Mater. Struct. 38 (2015) 503–517.
[35] Seweryn, A., Poskrobko, S., Mróz, Z., Brittle fracture in plane elements with sharp notches under mixed-mode loading, J. Eng. Mech. 123 (1997) 535-543.
[36] Kihara, S., Yoshii, A., A strength evaluation method of a sharply notched structure by a new parameter, "The Equivalent Stress Intensity Factor". JSME Int. J., 34 (1991) 70-75.
[37] Livieri, P., Lazzarin, P., Notch Stress Intensity Factors and fatigue strength of aluminium and steel welded joints, Int. J. Fract. 133 (2005) 247-276.
[38] Atzori, B., Dattoma, V., A comparison of the fatigue behaviour of welded joints in steels and in aluminium alloys, IIW Doc XXXIII (1983) 1089-1983.
[39] Haibach, E., Service Fatigue-Strength – Methods and data for structural analysis. Dusseldorf, VDI (1989).
[40] Lazzarin, P., Berto, F., Gomez, F.J., Zappalorto, M., Some advantages derived from the use of the strain energy density over a control volume in fatigue strength assessments of welded joints, Int. J. Fatigue, 30 (2008) 1345-1357.
[41] Lazzarin, P., Berto, F., Zappalorto, M., Rapid calculations of notch stress intensity factors based on averaged strain energy density from coarse meshes: Theoretical bases and applications, Int. J. Fatigue, 32 (2010) 1559–1567.
[42] Meneghetti, G., Campagnolo, A., Berto, F., Atzori, B., Averaged strain energy density evaluated rapidly from the singular peak stresses by FEM: cracked components under mixed-mode (I+II) loading, Theor. Appl. Fract. Mech., 79 (2015) 113–124.
[43] Gallo, P., Berto, F., Glinka, G Generalized approach to estimation of strains and stresses at blunt V-notches under non-localized creep, Fatigue Fract. Eng. Mater. Struct 39 (2016), 292-306.